Nanoscale

Accepted Manuscript

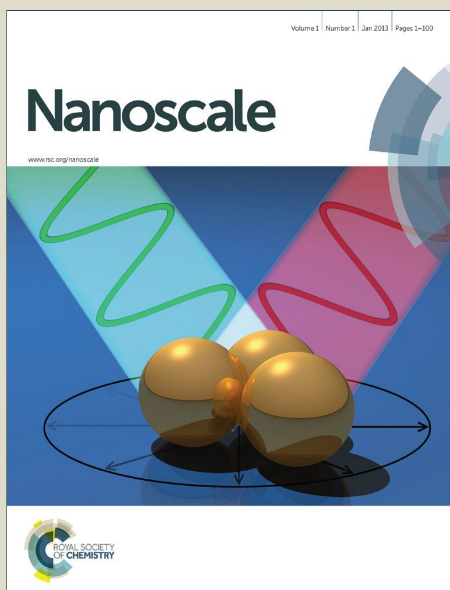

This is an *Accepted Manuscript*, which has been through the Royal Society of Chemistry peer review process and has been accepted for publication.

Accepted Manuscripts are published online shortly after acceptance, before technical editing, formatting and proof reading. Using this free service, authors can make their results available to the community, in citable form, before we publish the edited article. We will replace this *Accepted Manuscript* with the edited and formatted *Advance Article* as soon as it is available.

You can find more information about *Accepted Manuscripts* in the Information for Authors.

Please note that technical editing may introduce minor changes to the text and/or graphics, which may alter content. The journal's standard Terms & Conditions and the Ethical guidelines still apply. In no event shall the Royal Society of Chemistry be held responsible for any errors or omissions in this *Accepted Manuscript* or any consequences arising from the use of any information it contains.

ROYAL SOCIETY OF CHEMISTRY

www.rsc.org/nanoscale

Journal Name

ARTICLE TYPE

Cite this: DOI: 10.1039/xxxxxxxxxx

Nanocrystal size distribution analysis from transmission electron microscopy images†

Martijn van Sebille,*[a] Laurens J. P. van der Maaten,[b] Ling Xie,[c] Karol Jarolimek,[a] Rudi Santbergen,[a] René A. C. M. M. van Swaaij,[a] Klaus Leifer,[c] and Miro Zeman[a]

Received Date
Accepted Date

DOI: 10.1039/xxxxxxxxxx

www.rsc.org/journalname

We propose a method with minimal bias caused by user input to quickly detect and measure the nanocrystal size distribution from transmission electron microscopy (TEM) images using a combination of Laplacian of Gaussian filters and non-maximum suppression. We demonstrate the proposed method on bright-field TEM images of an a-SiC:H sample containing embedded silicon nanocrystals with varying magnifications and we compare the accuracy and speed with size distributions obtained by manual measurements, a thresholding method and PEBBLES. Finally, we analytically consider the error induced by slicing nanocrystals during TEM sample preparation on the measured nanocrystal size distribution and formulate an equation to correct for this effect.

Nanoscale Accepted Manuscript

1 Introduction

Silicon nanocrystals embedded in a high band gap Si-rich alloy form interesting materials that can be used as top cells of multi-junction solar cells. The band gap of these materials can be tuned by the nanocrystal size.[1] This allows to minimize thermalization losses and thereby increase the solar-cell efficiency. The mean and deviation of nanocrystal size are crucial parameters in determining the optical properties of the material,[2,3] and electronic transport properties in photovoltaic devices.[4] Furthermore, for silicon nanocrystals with a sufficiently narrow size distribution and which are closely spaced, a miniband will form and result in an increase of the effective band gap of the superlattice material.[5] Therefore, controlling both the mean size and the size distribution of silicon nanocrystals is of great importance.

Limited by the nanometer-scale dimensions of nanocrystals, transmission electron microscopy (TEM) is the only direct measurement tool capable of capturing the size and shape of embedded nanocrystals. Although silicon nanocrystal size distributions obtained from TEM images have been reported (e.g. Ref[3,6,7,8]), the method used to obtain these distributions is either unclear, performed using closed source software or without the possibility to verify which nanocrystals were measured.

When we consider nanocrystals of different materials, we find more and clearer methods are used, but all lack either in analysis speed, accuracy, or both. These analyses are typically carried out manually or by thresholding methods (e.g. Ref[9,10,11]). Manual measuring is very time-consuming and can be biased by subjective choices and expectations. Thresholding methods face difficulties when applied to images with background inhomogeneities. These methods typically need high quality TEM images with high signal-to-noise ratios and homogeneous backgrounds to function properly. Furthermore, poor choice of threshold settings might lead to biased results.[12]

A different approach was reported by Mondini *et al.* They demonstrated PEBBLES, a method based on fitting each nanocrystal individually with an intensity profile.[13] This method is not sensitive to inhomogeneous background or global contrast differences. However, with an analysis speed of 1 nanocrystal/s under favorable conditions and significantly slower speeds for sub-optimal conditions[13] analyzing several images with hundreds of nanocrystals is time-consuming. So, a quick method to measure nanocrystals in TEM images with minimal user input to minimize user bias has been lacking.

We propose a semi-automatic method to quickly measure the

[a] *Photovoltaic Materials and Devices, Delft University of Technology, Mekelweg 4, 2628 CD Delft, The Netherlands; E-mail: m.vansebille@tudelft.nl*
[b] *Pattern Recognition Laboratory, Delft University of Technology, Mekelweg 4, 2628 CD Delft, The Netherlands*
[c] *Applied Materials Science, Uppsala University, Ångströmlab, Lägerhyddsvägen 1, 752 37 Uppsala, Sweden*

† Electronic Supplementary Information (ESI) available: [details of any supplementary information available should be included here]. See DOI: 10.1039/b000000x/

sizes of nanocrystals in any type of TEM image in order to obtain the nanocrystal size distribution, using a combination of Laplacian of Gaussian (LoG) filters, non-maximum suppression, and a boundary overlay. The only user input required is a minimum and a maximum nanocrystal size, and a non-maximum suppression threshold value. After applying the automated part of the method, the user is able to judge the quality of the result in a manual verification step. We also show in this paper that these parameters can be determined for one image and then be accurately used in similar images. Furthermore, we analytically consider the effect of slicing nanocrystals during sample preparation on the nanocrystal distribution as measured with TEM. We establish equations describing this effect and propose a simple method to correct for it.

This paper is organized as follows. We first describe the experimental details under which the sample was fabricated and measured in section 2. Next, we describe the principles and mathematics behind the developed method in section 3 and we go through the method step by step, demonstrating the steps on a small section of a bright-field TEM (BF-TEM) image. The results of applying our method on a validation and several testing images is shown in section 4. Finally we validate the method and show that the method parameters can be safely transfered between similar images in section 5.

2 Experimental details

All TEM images were made on the same sample. We deposited a-$Si_{0.71}C_{0.29}$:H on quartz substrates from G.M. Associates in a radio frequency plasma-enhanced chemical vapor deposition reactor operating at 13.56 MHz. The sample was deposited and annealed with the following deposition parameters: a power density of $0.139\,\mathrm{W\,cm^{-2}}$, substrate temperature of 360 °C, and SiH_4 and CH_4 flows of 10.2 sccm and 91.8 sccm, respectively. After deposition the sample was annealed in a furnace at 1100 °C for 60 min.

TEM measurements were performed using a FEI TECNAI F30ST microscope equipped with a field emission gun operated at 300 keV. Conventional TEM sample preparation techniques including mechanical polishing and grazing incidence (6°, 5 kV) Ar-ion milling was used to obtain samples in plan-view geometry.

All computer assisted analyses were performed on a computer with Intel Core2 Quad CPU at 2.66 GHz, with 4 GB RAM and 64-bit operating system, using MATLAB R2015A.

3 Theory, method and distribution correction

3.1 Theory

The analysis method is based on the application of Laplacian of Gaussian (LoG) filters, which are commonly used in image processing.[14,15,16] These filters are blob-detectors which respond to circular image structures with certain sizes, determined by their scale parameters. This makes these filters very suitable for the detection of nanocrystals in TEM images. LoG filters combine a Gaussian and Laplacian filter in one. The Gaussian filter G serves to reduce noise by smoothing the image and is given by:

$$G(x,y,\sigma) = \frac{1}{2\pi\sigma^2}\exp\left(-\frac{x^2+y^2}{2\sigma^2}\right), \quad (1)$$

where x and y are the two dimensions of the image, and σ is the scale parameter. The Laplacian filter is the sum of the second spatial derivative in x- and y-directions, and calculates the local curvature of intensities in the image $I(x,y)$ and is given by:

$$L(x,y) = \frac{\partial^2 I}{\partial x^2} + \frac{\partial^2 I}{\partial y^2}. \quad (2)$$

Combining these two filters results in the second spatial derivative of the Gaussian filter, or Laplacian of Gaussian filter $\nabla^2 G$:

$$\nabla^2 G(x,y,\sigma) = \frac{\partial^2 G}{\partial x^2} + \frac{\partial^2 G}{\partial y^2}. \quad (3)$$

An example of a LoG filter is shown in figure 1. The scale

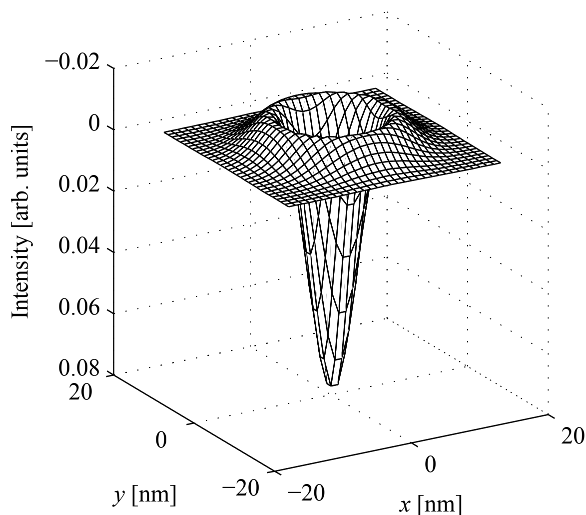

Fig. 1 A normalized LoG filter with $\sigma = 8$ nm.

parameter σ determines the width of the LoG filter in x- and y-dimensions. A range of LoG filters with different scale parameters is applied. All possible scales within this range are referred to as the scale space. The scale space is sampled linearly, since the nanocrystal size distributions are expected to be relatively narrow, spanning one or at most two orders of magnitude.

The intensity of the response of LoG filters is used in a later step to determine the position and size of the detected nanocrystals, as described in section 3.2.3. This response decreases as its scale parameter increases, so in order to prevent a bias towards smaller

Nanoscale Accepted Manuscript

This journal is © The Royal Society of Chemistry [year]

scales, the LoG filters are normalized by multiplying them with σ^2:[14]

$$\nabla^2_{norm} G(x,y,\sigma) = \sigma^2 \left(\frac{\partial^2 G}{\partial x^2} + \frac{\partial^2 G}{\partial y^2} \right), \tag{4}$$

where $\nabla^2_{norm} G(x,y,\sigma)$ is the normalized Laplacian of Gaussian (NLoG) filter. NLoG filters are applied by convoluting the original image $I(x,y)$ with the NLoG filter $\nabla^2_{norm} G$, resulting in a three-dimensional response image $f(x,y,\sigma)$[15]:

$$f(x,y,\sigma) = \nabla^2_{norm} G(x,y,\sigma) * I(x,y). \tag{5}$$

The response of an NLoG filter achieves a maximum amplitude at the center of the nanocrystal, provided the scale of the NLoG filter matches the scale of the nanocrystal. For disks, this is the case when the zero-crossing of an NLoG filter overlaps with the edge of the nanocrystal and can be expressed as $\sigma = r/\sqrt{2}$, where r is the nanocrystal radius in the TEM image. However, for the intensity profiles of nanocrystals in amorphous silicon alloys this is not the case, shown in figure 2. The ratio between a nanocrystal radius

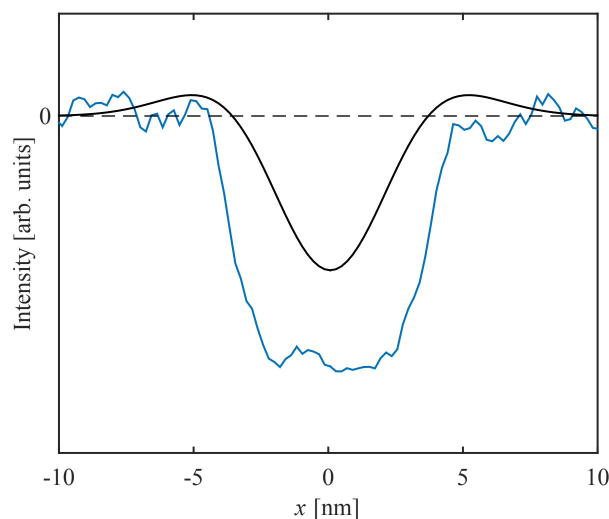

Fig. 2 1D intensity profile of a nanocrystal with radius of 4.2 nm (blue line), the LoG filter corresponding to the maximum intensity response, with σ of 2.53 nm (black solid line) and zero intensity (black dashed line).

and its matching scale parameter was obtained using the validation image (see section 4.1). The ratio was determined for all correctly detected nanocrystals (the number of detected nanocrystals minus false positives) and was found to be 1.52 ± 0.113, so:

$$\sigma = \frac{r}{1.52}. \tag{6}$$

This will be used in section 3.2.2.

3.2 Method

The semi-automatic method consists of a series of steps in order to quickly determine the position and nanocrystal size distribution within a TEM image. These steps are:

1. **Preprocessing** of the image
2. **Convolution of TEM image with NLoG filters** within a sampled scale space
3. **Determining the position and characteristic scale of nanocrystals** by finding the local maximums in the 3D NLoG response and subsequent application of non-maximum suppression
4. **Verification** of analysis by overlaying the obtained nanocrystal positions and boundaries on the original TEM image

These steps will be discussed in more detail below. The method is available as MATLAB code as Electronic Supplementary Information.†

3.2.1 Preprocessing.

During preprocessing the contrast of a raw TEM image is adjusted for two purposes. The first is to make the contrast profiles similar for the different TEM images. This allows us to determine the optimal non-maximum suppression threshold value, as described in section 3.2.3, and directly apply it to comparable TEM images. The second reason is to ensure the user can clearly distinguish the nanocrystals from the background, allowing the user to verify whether the method worked correctly, as described in section 3.2.4. Preprocessing is realized by normalizing the intensity of the image $I(x,y)$ and subsequently changing the contrast to match a normally distributed histogram with mean and standard deviation of 0.5 and 0.1, respectively. This is achieved by a gray-scale transformation T to minimize

$$|c_1(T(k)) - c_0(k)|, \tag{7}$$

where c_0 is the cumulative histogram of $I(x,y)$ and c_1 is the cumulative sum of the normally distributed histogram for all intensities k.[17] The result is that all images have comparable contrast. Note that all analyses were performed after these preprocessing steps, except for the PEBBLES method, which uses the original TEM image.

3.2.2 Convolution with NLoG filters.

The scale space range is determined by estimating the range of nanocrystal radii in the TEM image. The smallest expected nanocrystal size is determined by an optimization using the validation image, described in section 4.1. The step size in expected nanocrystal radii is set by an increment of 1 pixel and the largest nanocrystal radius is estimated by the user. The largest

Nanoscale Accepted Manuscript

nanocrystal can be estimated by manually guessing or measuring the largest nanocrystal in a given image. The expected range of nanocrystal sizes is then multiplied by 0.6, according to equation 6 to obtain the sampled scale space. Note that when the largest nanocrystal radius to be detected is set too small, the biggest nanocrystals will not be detected correctly, resulting in a bias towards smaller nanocrystals. However, this can be verified quickly in the verification step, discussed in section 3.2.4. When the largest nanocrystal is set too big, computation times will increase and there is a risk of incorrectly detecting other, larger features, should there be any. When the smallest nanocrystal radius to be expected is set too small, there is a risk of falsely detecting noise as nanocrystals. Alternatively, when the smallest expected nanocrystal size is too large, the smallest nanocrystals might not be detected and there might be a bias towards bigger nanocrystals.

To illustrate this step, we consider a small section of a BF-TEM image, shown in figure 3a, containing several small nanocrystals and a bigger nanocrystal near the top of the image. Figures 3b and 3c show the result of the convolutions of the original TEM image with NLoG filters with scales of 1.9 nm and 4.3 nm, respectively. The result of the small NLoG filter, shown in figure 3b, is that the contrast for the small nanocrystal (labeled B) is enhanced. Also note that the bigger nanocrystal (labeled A) results in a relatively low intensity. Since the background noise feature size is quite close to the size of the smallest nanocrystals, the background noise is also enhanced to some extent, although not as significantly as the small nanocrystals. The result of the larger NLoG filter, shown in figure 3c, is that the largest nanocrystal A is enhanced with the highest image intensity in its center. The smaller nanocrystals are also detected, but their intensity is lower, indicating that the scale parameter of this NLoG filter is not the best match for these nanocrystals.

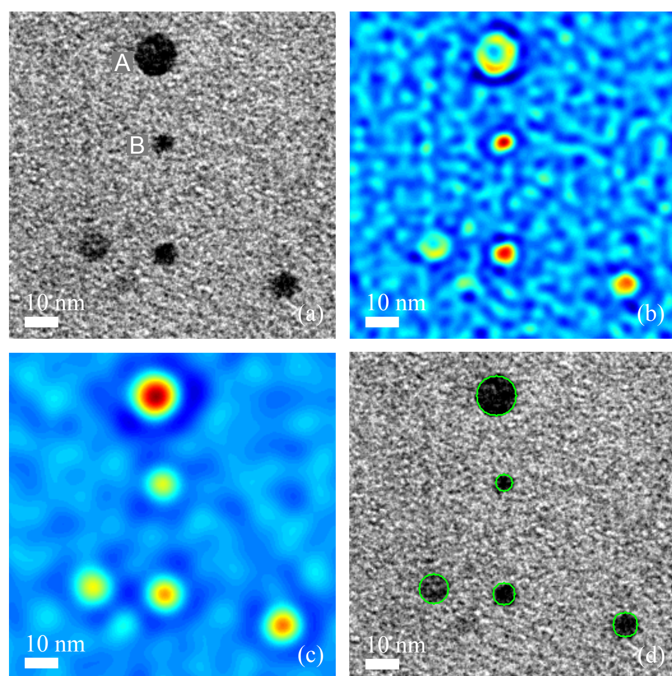

Fig. 3 (a) A section of a BF-TEM image with several nanocrystals of different sizes. The result of the convolutions of the original image with NLoG filters with σ of 1.9 nm (b) and 4.3 nm (c), corresponding to nanocrystal radii of 2.9 nm and 6.5 nm, respectively. Figures (b) and (c) are displayed with the same color scale, which indicates the intensity of the resulting response image $f(x,y,\sigma)$, see equation 5. (d) Nanocrystals encircled to verify correct identification of nanocrystals.

3.2.3 Determining the position and characteristic scale of nanocrystals.

Next, non-maximum suppression (NMS) is applied to simultaneously determine the nanocrystal position and size, and to discard noise. This is achieved by finding the local maximum values in the three-dimensional response image $f(x,y,\sigma)$, from equation 5. In order to prevent the false detection of noise as nanocrystals, a maximum is only considered as such when it is the maximum value within its local $5\times5\times5$ pixel-subset of the three-dimensional array and if its value is equal to or larger than the NMS threshold. The physical size of 5 pixels depends on the pixel size of the TEM image and ranges between 1.035 nm to 2.880 nm for the images used in this study.

The first of these two conditions causes only the best scale space-nanocrystal match to show up as a maximum. If we consider figure 3c, we see that a scale parameter of 4.3 nm enhances the smallest nanocrystal (labeled B), with its center the local intensity peak in the (x,y) plane. However, in scale space, it is not the maximum, since figure 3b shows the same nanocrystal with higher intensity. In scale space, the intensity at that position will change and peak at the best scale space-nanocrystal match.

The second requirement, stating that each intensity peak in the local $5\times5\times5$ sub-array should at least be as high as the NMS threshold value, discards noise. Figures 3b and 3c show several lower intensity peaks due to background noise. These peaks might have a local maximum at some scale parameter, but they are not nanocrystals. The NMS threshold prevents the noise from being detected as nanocrystals. The NMS threshold value influences the outcome of the procedure significantly and could lead to inaccurate results if applied incorrectly. However, we will show that this threshold can be determined for one type of TEM image and can then be safely and correctly applied to similar TEM images, limiting user-caused bias. Furthermore, the next step is used to manually verify the outcome of the automated method and an incorrect value will be clear.

Nanoscale Accepted Manuscript

This journal is © The Royal Society of Chemistry [year]

3.2.4 Verification.

After obtaining a three-dimensional array with nanocrystal position and size, the outcome can be verified by overlaying the results with the original TEM image, as shown in figure 3d. This allows for a quick verification of the applied parameters and shows whether anything has been set incorrectly. A too low value for the largest nanocrystal would reveal the biggest nanocrystals not encircled. When the NMS threshold parameter is set too low, noisy background peaks will be encircled and when set too high, some nanocrystals will not be encircled.

3.3 Distribution correction

During TEM sample preparation the sample is thinned to several tens of nanometers. When the sample thickness t approaches the size of nanocrystals, the chance of slicing a significant number of nanocrystals increases and thus the measured nanocrystal size distribution will get distorted. For simplicity, we will assume all nanocrystals are spherically shaped. When a nanocrystal is depicted in a TEM image, we observe its two-dimensional projection of the three-dimensional spherical nanocrystal.

There are three cases we should consider: (i) when the nanocrystal's center is inside the sample, (ii) when its center is less than R outside the sample, and (iii) when the nanocrystal's center is more than R outside the sample. Since we observe the nanocrystal's 2D projection, and we are using transmission measurements, for case (i) the apparent radius r is the same as its true radius R and will show up as such in the TEM image, as shown schematically in figure 4a. However, when a nanocrystal is sliced

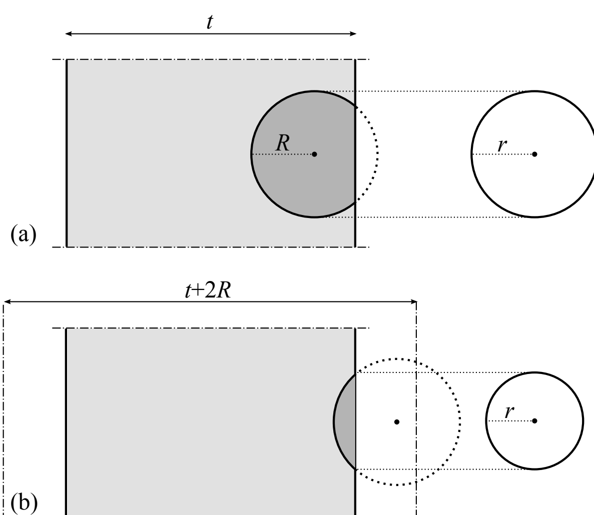

Fig. 4 Schematic of a sample (light gray) with a nanocrystal (dark gray), with its center (•) inside the sample (a) and up to R outside the sample (b)

during sample preparation and its center is located up to R outside the sample (case ii), the apparent radius R will differ from r, as shown in figure 4b. The third case, when a nanocrystal is located more than R outside the sample (case iii), it will not be measured at all. We assume that the nanocrystals are distributed randomly throughout the sample. Nanocrystals that show up in TEM images have their center located within $t+2R$. With this, the probability $P_{outside}$ of a nanocrystal's center for a given nanocrystal in the image being located up to R outside the sample, can be expressed as follows:

$$P_{\text{outside}}(t,R) = \frac{2R}{t+2R}. \quad (8)$$

The probability of a nanocrystal's center being located inside the sample is then:

$$P_{\text{inside}}(t,R) = 1 - \frac{2R}{t+2R} = \frac{t}{t+2R}. \quad (9)$$

If a nanocrystal, shown schematically in figure 5, is sliced it happens at a random position, so every position x is equally likely. The probability density function $f_{apparent}$ of finding an apparent

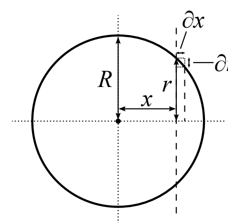

Fig. 5 A nanocrystal shown schematically.

radius r is then:

$$f_{\text{apparent}}(r) = C\frac{\partial x}{\partial r}, \quad (10)$$

where C is a normalization constant. According to Pythagoras' theorem:

$$x^2 + r^2 = R^2, \quad (11)$$

which can be rewritten to:

$$x = \pm\sqrt{R^2 - r^2}. \quad (12)$$

After finding and replacing the normalization constant in equation 15, the positive and negative versions of equation 12 both lead to equation 16. For simplicity we will continue the derivation with only the negative one. This leads to the following derivative:

$$\frac{\partial x}{\partial r} = \frac{-r}{\sqrt{R^2 - r^2}}. \quad (13)$$

Combining equations 10 and 13 gives:

$$f_{\text{apparent}}(r) = C\frac{-r}{\sqrt{R^2 - r^2}}. \quad (14)$$

Nanoscale Accepted Manuscript

The normalization constant C can be found by equating:

$$\int_0^R f_{\text{apparent}}(r)\,\mathrm{d}x = 1 \rightarrow C = \frac{-1}{R}. \quad (15)$$

Combining equations 14 and 15 leads to:

$$f_{\text{apparent}}(r) = \frac{r}{R\sqrt{R^2 - r^2}}. \quad (16)$$

The probability $P_{apparent}$ of finding a nanocrystal with apparent radius r in the interval $a \leq r \leq b$ can then be calculated with:

$$P_{\text{apparent}}(r) = \int_a^b \frac{r}{R\sqrt{R^2 - r^2}}\,\mathrm{d}r. \quad (17)$$

For a nanocrystal with real radius of 5 nm, the result is shown in figure 6. The apparent radius for a nanocrystal measured by TEM

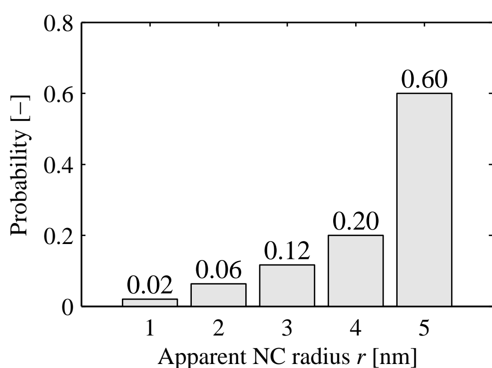

Fig. 6 Probability of finding apparent radius r for real radius R of 5 nm, when the nanocrystal is sliced at a random position.

depends on the real radius R and the sample thickness t and by combining equations 8, 9 and 17 can be written as follows:

$$r(R,t) = R\left[\frac{2R}{t+2R}\int_0^R \frac{r}{R\sqrt{R^2-r^2}}\,\mathrm{d}r + \frac{t}{t+2R}\right]. \quad (18)$$

This equation can be used on a known nanocrystal size distribution in order to calculate the distribution of apparent radius r, for a given sample thickness, as shown in figure 7. This figure shows that the apparent nanocrystal size distribution can be significantly different from its real nanocrystal size distribution, depending on the nanocrystal size and sample thickness. Greater nanocrystal radii and a thinner sample thickness leading to more distorted apparent size distributions.

In practice the real size distribution is unknown. From TEM images we can obtain the size distribution of apparent radii and from the sample preparation we can get a close approximation of the sample thickness. We can then fit the real nanocrystal size distribution using equation 18, thereby correcting for possible slicing of nanocrystals.

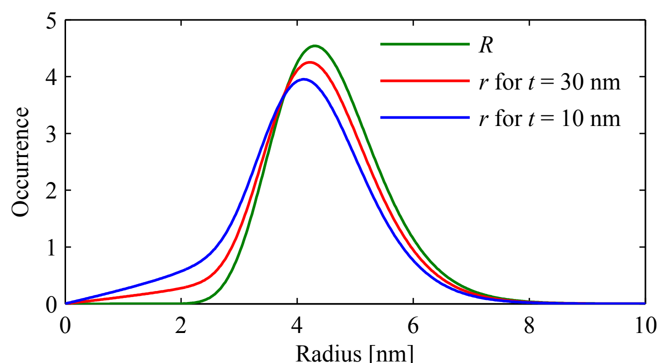

Fig. 7 A log-normally distributed real nanocrystal radius R with $\mu = 1.5$ nm and $\sigma = 0.2$ nm (green) and apparent radius distribution r for sample thickness of 30 nm and 10 nm shown in red and blue, respectively.

4 Results

The proposed method to determine the nanocrystal size distribution will be demonstrated and tested as follows. It will be calibrated using a validation image, a BF-TEM image, shown in figure 8. This image will be used to determine the NMS threshold value and maximum nanocrystal size in section 4.1. This image has a relatively homogeneous background and high contrast between nanocrystals and background, making it easy to manually annotate the nanocrystals and to calibrate the proposed method. Next, using these parameters the method will be applied on a test set in section 4.2. The accuracy of the results on the test set is a measure of the quality of the method proposed.

Since the nanocrystal size distribution of any sample is not known a priori, there is no objective way to evaluate the performance of such an analysis method. Therefore we compare the results of our proposed method with a size distribution obtained by manually annotating all nanocrystals in the image. We assume that the nanocrystals annotated manually are correct, which implies that nanocrystals found automatically with the NLoG method, but not manually are false positives and vice versa are false negatives. The false positives and false negatives can be expressed as percentages of the total number of nanocrystals found with manual annotation in the image to indicate the accuracy of the method. In addition to the accuracy in detecting nanocrystals, there should not be a significant bias toward smaller or larger nanocrystals detected. The nanocrystal diameter found with the automated method should correspond with the actual nanocrystal size. The obtained size distribution should be accurate and represent the actual nanocrystal size distribution. Therefore we compare the obtained size distribution with the size distribution obtained from manual annotation of the nanocrystals. We also compare the mean nanocrystal size and mean absolute deviation of the size distribution. Additionally, we compare the results of our method to results obtained by `PEBBLES` and a

Nanoscale Accepted Manuscript

This journal is © The Royal Society of Chemistry [year]

thresholding method. PEBBLES was used with MATLAB R2014a and used according to the recommendations by Mondini *et al.* [13] It was calibrated for all three images individually before running the automated method. First 10 random nanocrystals were fitted manually using the spherical quadratic model. Subsequently the image was fit automatically with the same model, using the manually fitted average equivalent diameter and delta as guess diameter and delta value and a grid with default spacing, see Ref[13]. For the threshold method, all pixels with intensity values smaller than the threshold are considered to be part of a nanocrystal and all other pixels are background. As with the NLoG method, the threshold value was optimized for the validation image and subsequently used to analyze the test set.

4.1 Validation

The NMS threshold value and the smallest and largest nanocrystal radius are the three input parameters for the NLoG method. The largest nanocrystal in the validation image, shown in figure 8, is measured manually and is approximated to be 8 nm for the validation image. Setting a higher largest nanocrystal radius mainly increases computation time, but does not affect results significantly. In order to determine the optimal NMS threshold and smallest nanocrystal radius, these parameters were varied with the goal of minimizing the sum of false positives and false negatives. The minimum of the sum of false positives and false negatives for the validation image is at a NMS threshold value of 0.203 and smallest nanocrystal radius of 4 pixels.

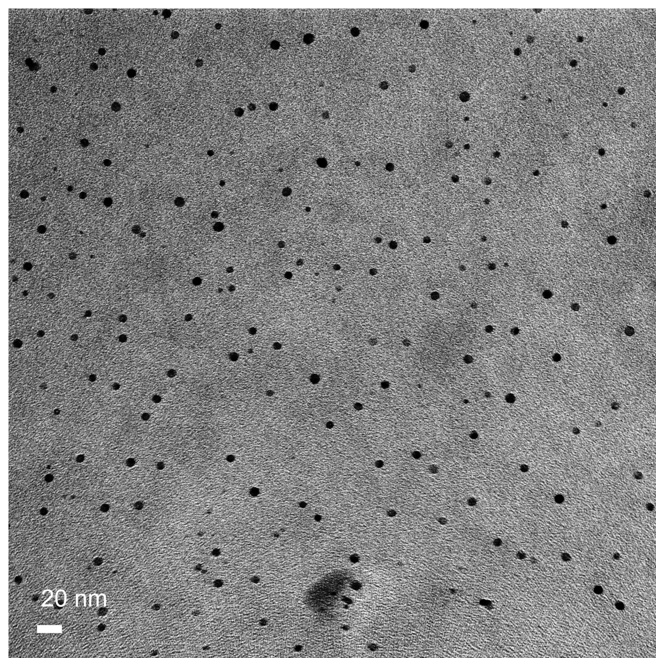

Fig. 8 BF-TEM image used as validation image, taken at $35\,000\times$ magnification and pixel size of 0.379 nm.

4.2 Test set

Next, the optimized parameters obtained from the validation image are applied on a test set, containing similar BF-TEM images.

4.2.1 Test image 1

The first is test image 1, taken at a lower magnification than the validation image and shown in figure 9a. This image has a background intensity gradient with a low-contrast region in the bottom-left corner and it has three nanocrystal clusters, which are encircled in white. The nanocrystals detected by the NLoG, PEBBLES and threshold methods are encircled in figures 9b–d, respectively. The NLoG method does not detect the nanocrystals in the low-contrast part of the image, while both PEBBLES and the threshold do detect some nanocrystals in this region. The NLoG method detects nanocrystals in the rest of the image as does PEBBLES. The thresholding method predominantly detects nanocrystals in the bottom-left corner and few in the rest of the image. NLoG correctly detects most nanocrystals in two of the three nanocrystal clusters, while the other two methods do not detect these nanocrystals.

The size distributions obtained by the manually annotated nanocrystals and the NLoG, PEBBLES and threshold method for test image 1 are shown in figure 10a–d, respectively. The nanocrystal distribution from manual annotation shows a single size distribution with an average size of approximately 4 nm. Both the NLoG and PEBBLES methods detect only the upper part of this size distribution. While PEBBLES shows a normal distribution, the NLoG method does not. Instead, it detected 270 nanocrystals with radii between 3.6 nm to 4.2 nm, corresponding to the smallest scale in the sampled scale space. The size distribution obtained with the threshold differs most from the distribution obtained by manual annotation.

The results of the different methods applied on test image 1 are listed in table 1.* The number of detected nanocrystals is the sum of correctly detected nanocrystals and false positives. The speed is defined as the number of correctly detected nanocrystals, which is the number of detected nanocrystals minus false positives, per second. The NLoG method detected most nanocrystals out of the three automated methods. It had the lowest number of false negatives, but still this was 21 % of the total number of nanocrystals. The mean nanocrystal radius measured by the NLoG method is

* The number of detected nanocrystals plus false negatives minus false positives does not (always) equal the number of detected nanocrystals using manual annotation. This is caused by touching nanocrystals. If nanocrystals touch in manual annotation, they are counted as a single nanocrystal. If they happen not to touch when detected automatically, they are then counted as two separate nanocrystals. The other way around can also occur.

Nanoscale Accepted Manuscript

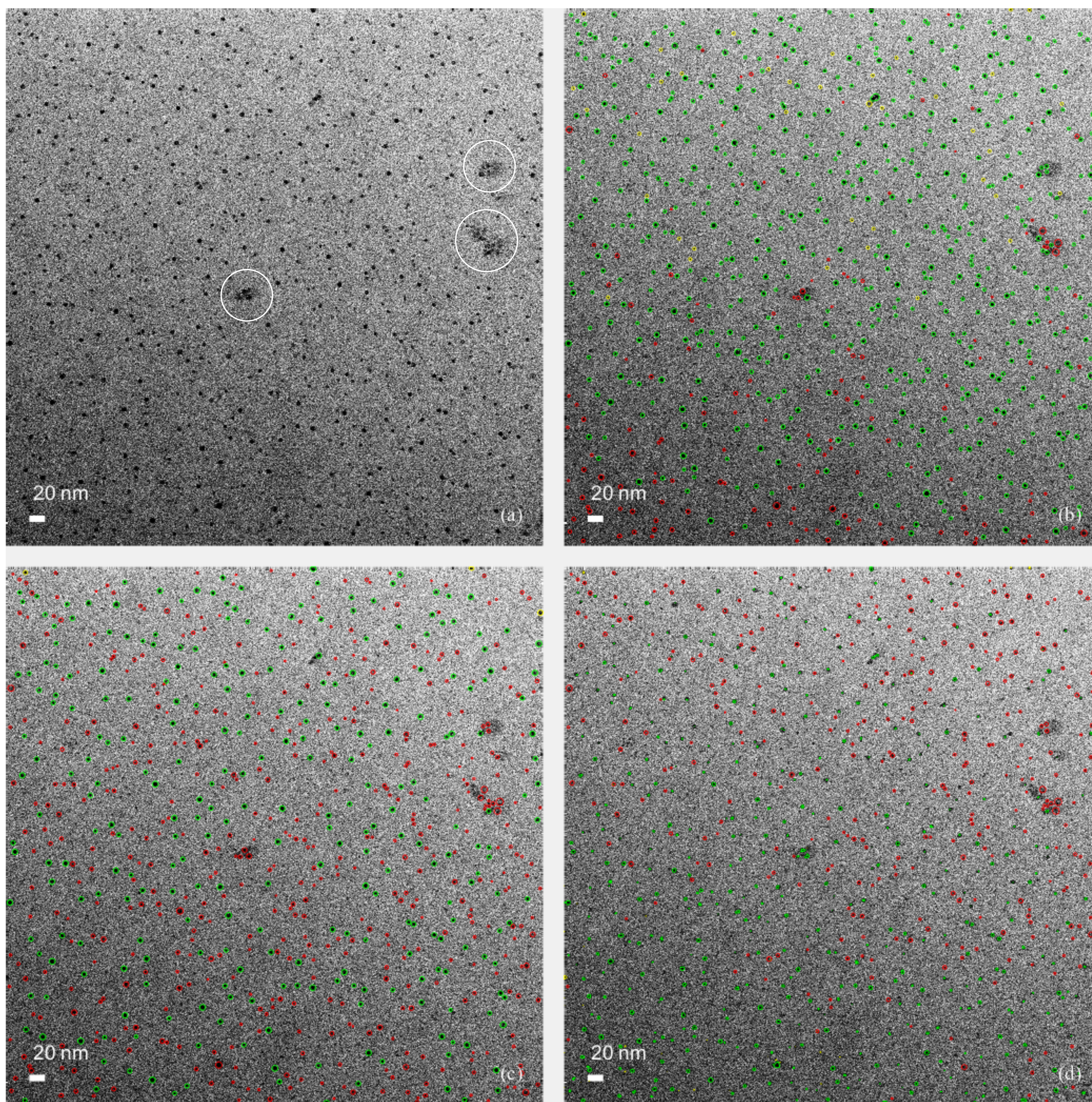

Fig. 9 (a) BF-TEM image used as test image 1, taken at $22\,500\times$ magnification and pixel size of $0.576\,\mathrm{nm}$. The three nanocrystal clusters are encircled in white. (b) The image with nanocrystals encircled detected using the NLoG method using a sampled scale space corresponding to nanocrystal radii of $4.6\,\mathrm{nm}$ to $8.6\,\mathrm{nm}$ ($2.3\,\mathrm{pixels}$ to $8.6\,\mathrm{pixels}$) and NMS threshold of 0.203, optimized for the validation image. (c) TEM image with nanocrystals encircled detected using `PEBBLES` with guess diameter of $15.4\,\mathrm{pixels}$, delta of -0.3937 and $99\,327\,\mathrm{grid}$ points spaced by 7.0. (d) TEM image with nanocrystals encircled detected using threshold with value of 0.099 optimized for the validation image. Nanocrystals encircled green, yellow and red indicate correctly detected nanocrystals, false positives and false negatives, respectively.

Nanoscale Accepted Manuscript

This journal is © The Royal Society of Chemistry [year]

Table 1 Results of manual annotation, NLoG, PEBBLES and threshold on test image 1

Method	Detected	False positives	False negatives	Mean r [nm] (error)	Mean absolute dev. [nm] (error)	Time [s]	Speed [s^{-1}]
Manual	770	-	-	3.98	0.82	8820	0.09
NLoG	644	39 (5.1 %)	160 (21 %)	4.27 (7.3 %)	0.65 (21 %)	96	6.3
PEBBLES	284	3 (0.4 %)	483 (63 %)	5.18 (30 %)	0.59 (27 %)	10683	0.03
Threshold	576	75 (9.7 %)	333 (43 %)	3.84 (3.4 %)	2.03 (148 %)	0.5	938

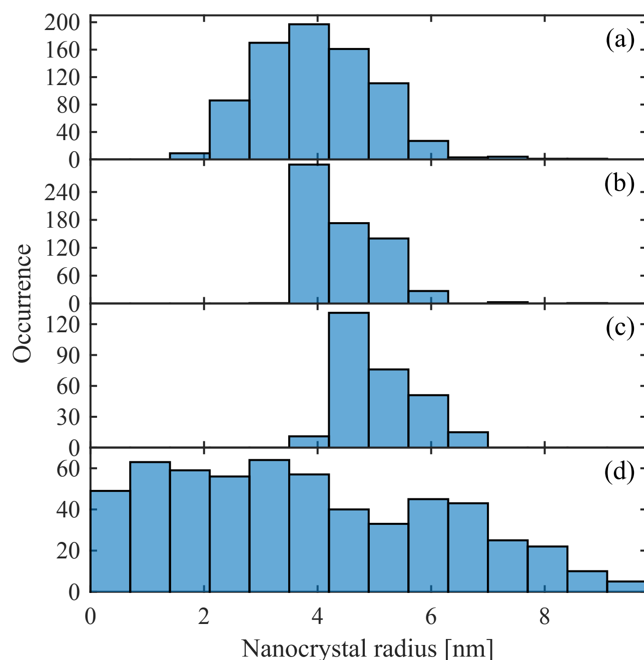

Fig. 10 Histogram of nanocrystal size distribution for test image 1, obtained from manual annotation of nanocrystals (a), NLoG method (b), PEBBLES (c) and threshold (d).

bigger than the mean radius obtained by manual annotation and differs by 7.3 %. The mean absolute deviation obtained with the NLoG method is closest to the one determined by manual annotation. The fastest method is the thresholding, followed by the NLoG method.

4.2.2 Test image 2

In the following we will analyze test image 2 (see figure 11a), which was taken at a greater magnification than the validation image. The nanocrystals detected by the NLoG, PEBBLES and threshold methods are encircled in figures 11b–d, respectively. The NLoG method correctly detects nanocrystals throughout the image, but did not detect some of the nanocrystals near the top edge of the image. PEBBLES did not detect a large number of nanocrystals throughout the image.

The size distributions obtained by the manually annotated nanocrystals and the NLoG, PEBBLES and threshold method for test image 2 are shown in figure 12a–d, respectively. A bimodal size distribution is obtained from manual annotation and the NLoG method matches this bimodal distribution closely. PEBBLES detected only nanocrystals with the smallest of the two size distributions, missing the larger of the nanocrystals. The thresholding method predominantly detected very small nanocrystals.

The results of the different methods applied on test image 2 are listed in table 2. The NLoG method generated 5.0 % false positives, while PEBBLES did not generate any false positives. The NLoG method had the lowest number of false negatives, however, compared to PEBBLES and threshold. Both the mean nanocrystal radius and mean absolute deviation obtained with the NLoG method are closest to their values obtained from manual annotation.

4.2.3 Test image 3

In order to illustrate the potential of the routine, we have also applied it on a more challenging image with irregular background and lower contrast, shown in figure 13a. A low-contrast region in the lowest left corner of the image is encircled in white. The nanocrystals detected by the NLoG, PEBBLES and threshold methods are encircled in figures 13b–d, respectively. The NLoG method performed reasonably well throughout the entire image, except for the low-contrast region. The number of false negatives for PEBBLES is considerably higher, but the method detected nanocrystals throughout the image, including the low-contrast re-

Nanoscale Accepted Manuscript

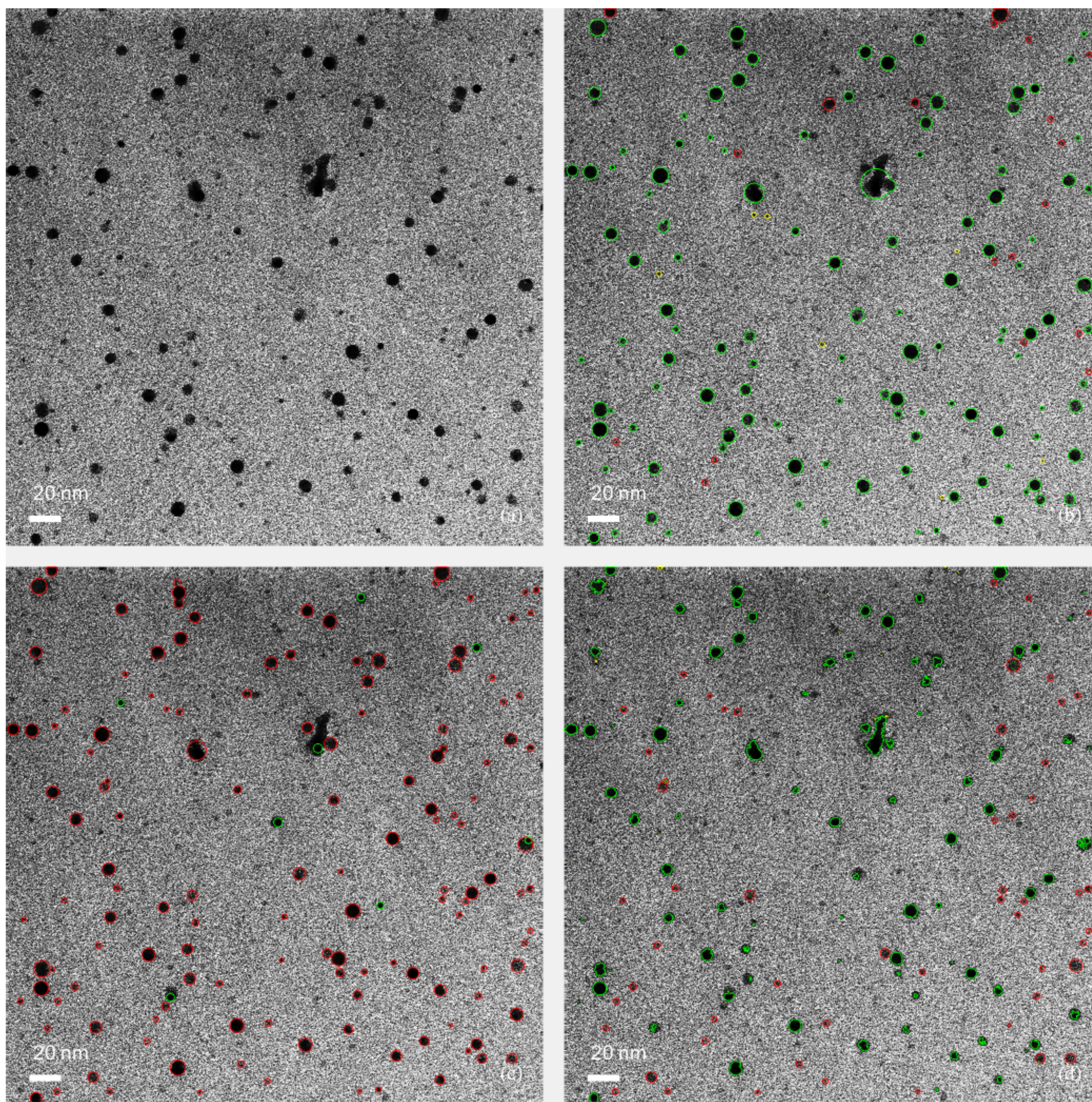

Fig. 11 (a) BF-TEM image used as test image 2, taken at $63\,000\times$ magnification and pixel size of $0.207\,\mathrm{nm}$. (b) The image with nanocrystals encircled detected using the NLoG method using a sampled scale space corresponding to nanocrystal radii of $0.83\,\mathrm{nm}$ to $7.88\,\mathrm{nm}$ ($4\,\mathrm{pixels}$ to $38\,\mathrm{pixels}$) and NMS threshold of 0.203, optimized for the validation image. (c) TEM image with nanocrystals encircled detected using PEBBLES with guess diameter of $23\,\mathrm{pixels}$, delta of -0.0073 and $40\,392$ grid points spaced by 11.0. (d) TEM image with nanocrystals encircled detected using threshold with value of 0.099 optimized for the validation image. Nanocrystals encircled green, yellow and red indicate correctly detected nanocrystals, false positives and false negatives, respectively.

Nanoscale Accepted Manuscript

This journal is © The Royal Society of Chemistry [year]

Table 2 Results of manual annotation, NLoG, PEBBLES and threshold on test image 2

Method	Detected	False positives	False negatives	Mean r [nm] (error)	Mean absolute dev. [nm] (error)	Time [s]	Speed [s^{-1}]
Manual	140	-	-	3.70	1.26	1800	0.08
NLoG	127	7 (5.0 %)	19 (14 %)	3.79 (2.5 %)	1.43 (14 %)	694	0.17
PEBBLES	8	0 (0.0 %)	133 (95 %)	3.10 (16.2 %)	0.31 (75 %)	4326	0.002
Threshold	162	21 (15 %)	53 (38 %)	3.48 (5.9 %)	1.26 (151 %)	0.1	1382

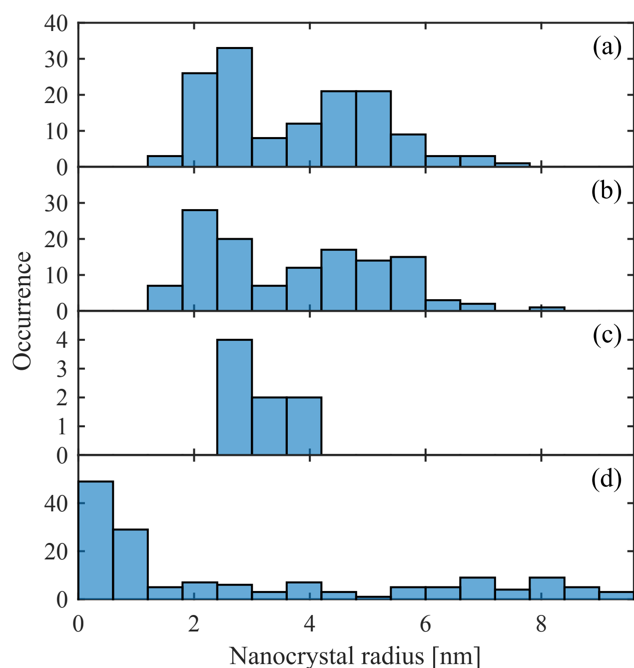

Fig. 12 Histogram of nanocrystal size distribution for test image 2, obtained from manual annotation of nanocrystals (a), NLoG method (b), PEBBLES (c) and threshold (d).

gion. The threshold method detected all nanocrystals correctly in the low-contrast region, but also generated most false positives. For the rest of the image, the threshold method detected some of the nanocrystals correctly.

The size distributions obtained by the manually annotated nanocrystals and the NLoG, PEBBLES and threshold method for test image 3 are shown in figure 14a–d, respectively. The nanocrystal distribution from manual annotation shows a single size distribution with an average size of approximately 3.6 nm. The NLoG method detected significantly more smaller sized nanocrystals than obtained from manual annotation, while the histograms match reasonably well for the larger nanocrystals. PEBBLES detected only the larger nanocrystals in the size distribution. The size distribution obtained with the threshold differs most from the distribution obtained by manual annotation.

The results of the different methods applied on test image 3 are listed in table 3. The NLoG method generated 47 % false positives, while PEBBLES did not generate any false positives. The NLoG method had the lowest number of false negatives, however compared to PEBBLES and threshold. Both the mean nanocrystal radius and mean absolute deviation obtained with the NLoG method are closest to their values obtained from manual annotation.

4.2.4 Nanocrystal slicing correction

The effect of nanocrystal slicing will be demonstrated on test image 2, since it was obtained at highest magnification of the test set and has a high contrast. Nanocrystal size distributions are typically considered to be log-normally distributed,[3,8] so in order to correct for slicing, the size distribution obtained by manual annotation was fit with a bimodal log-normal distribution, described by:

$$L(r) = p\frac{1}{rs_1\sqrt{2\pi}}\exp\left[-\frac{(\ln r-\mu_1)^2}{2s_1^2}\right] + (1-p)\frac{1}{rs_2\sqrt{2\pi}}\exp\left[-\frac{(\ln r-\mu_2)^2}{2s_2^2}\right]. \quad (19)$$

The histogram of nanocrystal sizes obtained by manual annotation for test image 2 and the histogram with nanocrystal sizes corrected for slicing are shown in figure 15. There is a distinct difference in the shape of the nanocrystal size distribution after

Nanoscale Accepted Manuscript

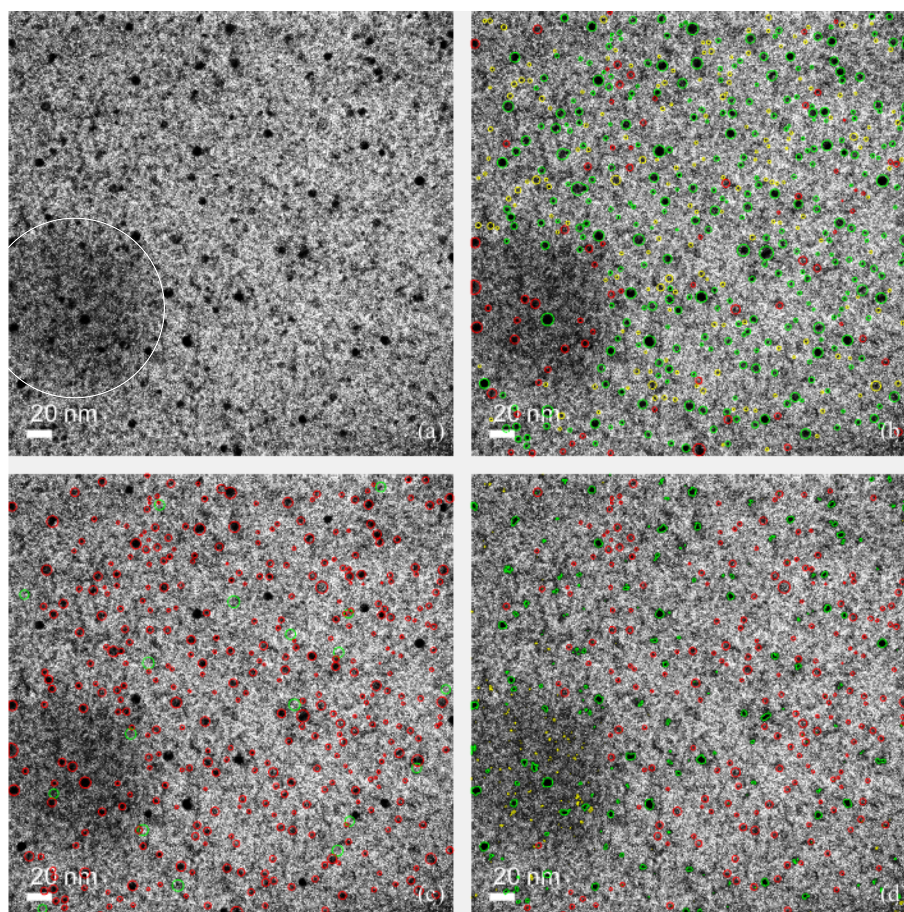

Fig. 13 (a) BF-TEM image used as test image 3, taken at $52\,000\times$ magnification and pixel size of $0.254\,\mathrm{nm}$. The low-contrast region is encircled in white. (b) The image with nanocrystals encircled detected using the NLoG method using a sampled scale space corresponding to nanocrystal radii of $1.02\,\mathrm{nm}$ to $5.85\,\mathrm{nm}$ ($4\,\mathrm{pixels}$ to $23\,\mathrm{pixels}$) and NMS threshold of 0.203, optimized for the validation image. (c) TEM image with nanocrystals encircled detected using `PEBBLES` with guess diameter of $39\,\mathrm{pixels}$, delta of -0.0052 and $13\,608\,\mathrm{grid}$ points spaced by 19.0. (d) TEM image with nanocrystals encircled detected using threshold with value of 0.099 optimized for the validation image. Nanocrystals encircled green, yellow and red indicate correctly detected nanocrystals, false positives and false negatives, respectively.

Nanoscale Accepted Manuscript

Table 3 Results of manual annotation, NLoG, `PEBBLES` and threshold on test image 3

Method	Detected	False positives	False negatives	Mean r [nm] (error)	Mean absolute dev. [nm] (error)	Time [s]	Speed [s^{-1}]
Manual	390	-	-	3.59	1.10	4500	0.09
NLoG	499	183 (47 %)	76 (19 %)	3.08 (14 %)	1.10 (0.3 %)	312	1.01
`PEBBLES`	19	0 (0 %)	370 (95 %)	5.93 (65 %)	0.52 (53 %)	2653	0.007
Threshold	475	203 (52 %)	219 (56 %)	2.21 (39 %)	1.84 (68 %)	0.2	1388

This journal is © The Royal Society of Chemistry [year]

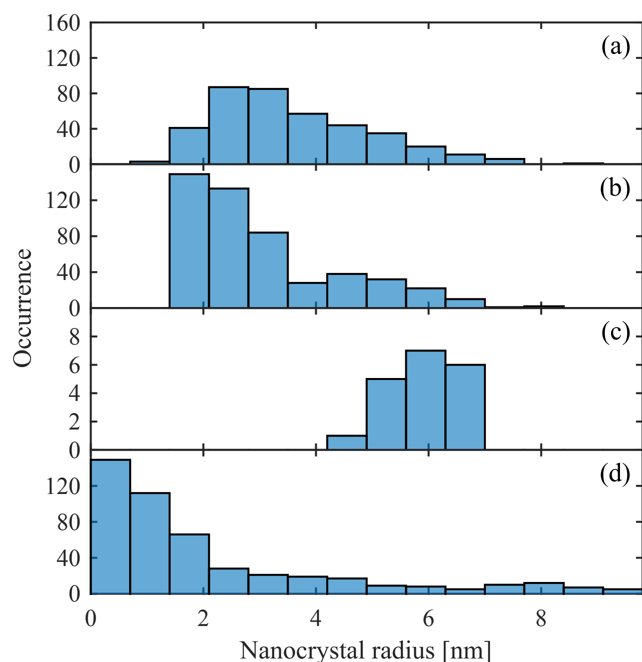

Fig. 14 Histogram of nanocrystal size distribution for test image 3, obtained from manual annotation of nanocrystals (a), NLoG method (b), PEBBLES (c) and threshold (d).

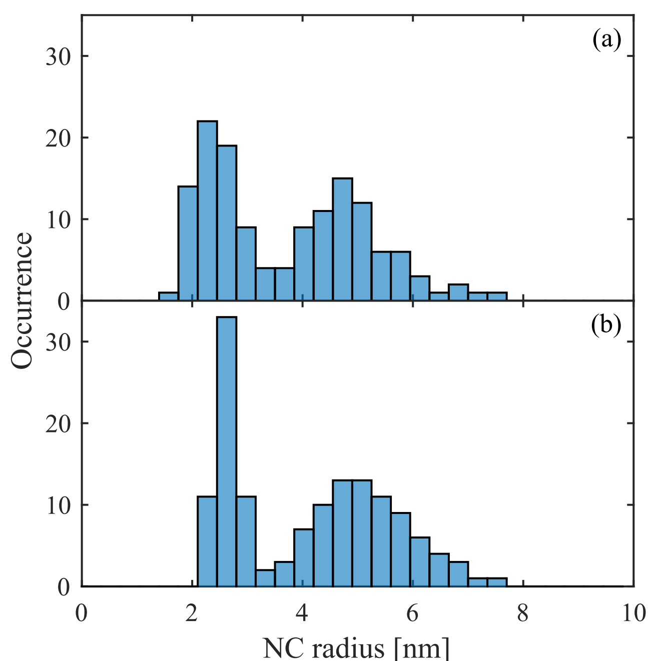

Fig. 15 (a) Histogram of uncorrected, apparent nanocrystal radii r for test image 2, obtained by manual annotation. (b) Histogram of the log-normal size distribution of real radii R that would, after correcting for slicing, best fit the measured apparent radii distribution. The sample thickness is assumed to be 25 nm, which is the sample target thickness during this sample's preparation.

correcting for nanocrystal slicing. The distribution parameters of the measured and corrected nanocrystal sizes are listed in table 4.

Table 4 Distribution parameters of measured apparent nanocrystal radii r and corrected real radii R on test image 2

Radius	Measured r	Corrected R
p [-]	0.476	0.399
μ_1 [nm]	0.864	0.893
s_1 [nm]	0.161	0.095
μ_2 [nm]	1.57	1.59
s_2 [nm]	0.180	0.185
Mean [nm]	3.70	3.96
Mean absolute deviation [nm]	1.26	1.26

The mean nanocrystal radius after correction for nanocrystal slicing is 7.1 % larger than the measured mean nanocrystal radius, while the mean absolute deviation after correction does not change significantly. Furthermore, the relative contribution of the bigger nanocrystals increased after correction, indicated by a lower p.

5 Discussion

Applying the three automated nanocrystal detection and measuring methods on the image test set, we can observe that all three methods have their own strengths and weaknesses. The threshold method is faster by at least two orders of magnitude than the fastest of the other methods. Its accuracy in false positives and false negatives and its accuracy in mean nanocrystal size and mean absolute deviation is low, however. Furthermore, the shape of the size distribution histograms differs most from the size distributions obtained by manual annotation.

PEBBLES is slowest for the images and settings used, even slower than manual annotation. It generated a negligible number of false positives, but the number of false negatives was highest of all methods in all test images. For all test images, the accuracy of PEBBLES in mean nanocrystal size was worst. For the unimodally distributed nanocrystal sizes of test image 1, its accuracy in mean absolute deviation was worse than the NLoG method, but not as bad as the threshold method. The histogram shape for test image 1 is similar to the one obtained by manual annotation, albeit right-shifted by approximately 1 nm. For test image 2, containing bimodally distributed nanocrystal sizes, PEBBLES failed to detect the larger nanocrystals. This resulted in 95 % false negatives and an error of 151 % for the mean absolute deviation. For test image 3 PEBBLES failed to detect the smaller nanocrystals, also resulting in 95 % false negatives.

The NLoG method performed best with regards to accuracy of mean nanocrystal size and mean absolute deviation for all three test images and for test image 2 it accurately captured the histogram shape of the nanocrystal size distribution. It did not perform as well for test image 1, however. Although it detected a number of the small nanocrystals, it overestimated their sizes.

Nanoscale Accepted Manuscript

This is caused by the input parameters used in the NLoG method and the difference in pixel size between the validation image and this specific test image. The relevant NLoG input parameter for this case is the smallest value in the sampled scale space. Together with the NMS threshold this parameter distinguishes the smallest nanocrystals from background noise. A too small value would cause the method to falsely detect noise as nanocrystals, but a too large value will cause the method to fail to detect the smallest nanocrystals, or still detect them at a greater scale. The latter happened in test image 1. The NLoG method was optimized for an image at relatively high magnification, so the nanocrystals in that image are of relatively large sizes in pixels. The smallest value in the sampled scale space could therefore be relatively large, minimizing false positives. Applying these parameters on test image 1, with lower magnification and relatively small nanocrystals in pixels, resulted in many of the smallest nanocrystals being detected at the smallest scale in the sampled scale space. However, although the NLoG method performed worse in test image 1, its results were comparable or better than the other automated methods used. For test image 1 the magnification is so low that the smallest nanocrystals are of similar size as noise fluctuations. In that case the NLoG method does not perform very well. However, such a low magnification makes all methods of nanocrystal detection difficult, including manual annotation. For test image 3, the NLoG method captured the histogram shape of the nanocrystal size distribution reasonably well, although it falsely detected too many smaller-sized nanocrystals. Note that because of the greater sample thickness used for this image, its contrast is considerably worse and there is an increased probability of overlapping nanocrystals. This makes the analysis significantly harder, not only for the automated routines, but also for manual annotation. Since manual annotation is used as a benchmark for the routine's performance, uncertainty in the manual annotation's results, leads to greater uncertainty in the performance of the evaluated routines.

For the test image set we find that a greater TEM image magnification leads to increased accuracy for the NLoG method. However, this effect is expected to be limited, since the number of nanocrystals captured is lower for greater magnifications, increasing the statistical error of the obtained size distribution. Furthermore, the contrast generated in HR-TEM images is different from BF-TEM images. The contrast due to lattice fringes will dominate in HR-TEM images instead of the high-contrast black nanocrystals seen in BF-TEM images, possibly decreasing the effectiveness of the NLoG method. This may imply that there is an optimal magnification range for TEM images, in order to achieve the highest possible accuracy for the NLoG method. However, this is beyond the scope of this article.

Also note that although all TEM images were taken from the same sample, the obtained size distributions differ significantly. Since we have no reason to expect sample inhomogeneity, this difference is attributed to the different magnifications used during imaging and the related pixel sizes. Test image 1, taken at $22\,500\times$ magnification, shows a unimodal size distribution. The pixel size for this image is $0.576\,\text{nm}$, which means that the smallest nanocrystals, with diameters of $1\,\text{nm}$ to $2\,\text{nm}$ will span only 2 to $4\,\text{pixels}$. Such small features are easily lost in background noise. This implies that an image with such a magnification is ill-suited to measure the smallest of the nanocrystals, leading to a distortion of the obtained size distribution. In contrast, test image 2 shows a bimodal nanocrystal size distribution. This image was taken at a greater magnification of $63\,000\times$ and has a pixel size of $0.207\,\text{nm}$. This means that nanocrystals with $1\,\text{nm}$ to $2\,\text{nm}$ diameter show up as features of 5 to $10\,\text{pixels}$, which makes them much easier to distinguish from background noise. Since the magnification of test image 3 is greater than that of test image 1, its size distribution should be more accurate. However, the contrast and background inhomogeneity is significantly worse, making it harder to correctly distinguish nanocrystals from background noise and possibly distorting the obtained size distribution with false positives and false negatives.

We stress that it is very difficult, if not impossible to obtain the true size distribution from TEM images. Slicing nanocrystals alters the apparent size distribution and it is very hard to objectively detect and correctly measure all nanocrystals in an image. Manual annotation leads to a user bias and is time-consuming. The NLoG method leads to comparable results and takes significantly less time. For test image 2 we analytically corrected the nanocrystal size distribution for nanocrystal slicing. We find that the error in mean absolute deviation by the NLoG method is larger than the error induced by slicing, but the error for the mean size is smaller for the NLoG method than induced by slicing.

The NLoG method was optimized and tested for BF-TEM images, but can also be optimized for dark-field or high-resolution TEM images.

6 Conclusions

We have demonstrated the NLoG method to quickly detect and measure nanocrystals in a TEM image to obtain the nanocrystal size distribution with minimum user input. The method uses a convolution of the TEM image with NLoG filters. Furthermore, we show that the input parameters for this method can be optimized for one image and can then be applied to similar images with comparable or smaller pixel sizes, leading to accurate results. We compared the accuracy and speed of this method with other methods used in literature and the proposed method performed comparable or better in the image test set. Furthermore, we have developed an analytical correction for the effect of slicing nanocrystals during TEM sample preparation on the apparent nanocrystal size distribution. We derived an equation for the ap-

Nanoscale Accepted Manuscript

This journal is © The Royal Society of Chemistry [year]

parent nanocrystal size for a given real nanocrystal size. Assuming a certain nanocrystal distribution shape, this equation can be used to fit a real nanocrystal size distribution from a measured apparent size distribution.

Acknowledgments

We acknowledge financial support for this research from ADEM, A green Deal in Energy Materials of the Ministry of Economic Affairs of The Netherlands (www.adem-innovationlab.nl).

References

1 M. A. Green, E.-C. Cho, Y. Cho, Y. Huang, E. Pink, T. Trupke, A. Lin, T. Fangsuwannarak, T. Puzzer, G. Conibeer and R. Corkish, Proceedings of the 20th European Photovoltaic Solar Energy Conference and Exhibition, 2005, pp. 3–7.

2 J. Heitmann, F. Müller, M. Zacharias and U. Gösele, *Advanced Materials*, 2005, **17**, 795–803.

3 M. Künle, T. Kaltenbach, P. Löper, A. Hartel, S. Janz, O. Eibl and K.-G. Nickel, *Thin Solid Films*, 2010, **519**, 151–157.

4 B. Puthen-Veettil, R. Patterson, D. König, G. Conibeer and M. A. Green, *J. Appl. Phys.*, 2014, **116**, 163707.

5 G. Conibeer, I. Perez-Wurfl, X. Hao, D. Di and D. Lin, *Nanoscale Research Letters*, 2012, **7**, 193.

6 V. Osinniy, S. Lysgaard, V. Kolkovsky, V. Pankratov and A. Nylandsted Larsen, *Nanotechnology*, 2009, **20**, 1–9.

7 Q. Cheng, E. Tam, S. Xu and K. K. Ostrikov, *Nanoscale*, 2010, **2**, 594–600.

8 I. F. Crowe, M. P. Halsall, O. Hulko, A. P. Knights, R. M. Gwilliam, M. Wojdak and A. J. Kenyon, *J. Appl. Phys.*, 2011, **109**, 083534.

9 M. Sezgin and B. Sankur, *Journal of Electronic Imaging*, 2004, **13**, 146–168.

10 G. H. Woehrle, J. E. Hutchison, S. Ozkar and R. G. Finke, *Turk J Chem*, 2006, **30**, 1–13.

11 L. C. Gontard, D. Ozkaya and R. E. Dunin-Borkowski, *Ultramicroscopy*, 2011, **111**, 101–106.

12 W. D. Pyrz and D. J. Buttrey, *Langmuir*, 2008, **24**, 11350–11360.

13 S. Mondini, A. M. Ferretti, A. Puglisi and A. Ponti, *Nanoscale*, 2012, **4**, 5356–5372.

14 T. Lindeberg, *International Journal of Computer Vision*, 1998, **30**, 79–116.

15 D. Marr and E. Hildreth, *Proceedings of the Royal Society of London. Series B. Biological Sciences*, 1980, **207**, 187–217.

16 J. Canny, *Pattern Analysis and Machine Intelligence, IEEE Transactions on*, 1986, **PAMI-8**, 679–698.

17 R. Gonzalez and R. Woods, in *Digital Image Processing*, Prentice Hall, 2nd edn, 2002, ch. Image Enhancement in the Spatial Domain, pp. 75 – 103.

Nanoscale Accepted Manuscript